Hindawi
Journal of Sensors
Volume 2022, Article ID 9369543, 6 pages
https://doi.org/10.1155/2022/9369543

Research Article

Research on Navigation and Positioning of Electric Inspection Robot Based on Improved CNN Algorithm

Yingkai Long,[1] **Mingming Du**,[2] **Xiaoxiao Luo**,[1] **Siquan Li**,[1] **and Yuqiu Liu**[3]

[1]*State Grid Chongqing Electric Power Research Institute, Chongqing 401121, China*
[2]*State Grid Chongqing Electric Power Company, Chongqing 400013, China*
[3]*Nanjing Unitech Electric Power Co., Ltd., Nanjing 211100, China*

Correspondence should be addressed to Yingkai Long; 31115307@njau.edu.cn

Received 29 May 2022; Revised 29 June 2022; Accepted 30 June 2022; Published 12 July 2022

Academic Editor: Haibin Lv

Copyright © 2022 Yingkai Long et al. This is an open access article distributed under the Creative Commons Attribution License, which permits unrestricted use, distribution, and reproduction in any medium, provided the original work is properly cited.

In order to improve the visual navigation performance in complex environment, a robust visual navigation method for substation inspection robot is proposed in this paper. Based on the robustness of hexagonal cone model to light changes, this method can solve the squeezing problem of navigation path in complex environment and reduce the interference caused by external light factors. Based on HM preprocessed images, semantic segmentation is carried out with deep convolutional neural network to obtain global features, local features, and multiscale information of images, so as to effectively improve the network recognition accuracy. The results show that the images after HM color space transformation and grayscale reconstruction can compress the color space while preserving the edge details, which is beneficial to the semantic segmentation network for further scene road recognition. Because the original structure of the network is not adjusted and the corresponding preprocessing layer is added, the size of the network model is relatively increased, but the reasoning speed of the original network is significantly improved, which is 16.4% on average.

1. Introduction

As a direction for the development of future energy networks, smart grids have been extended to existing power grid control networks [1]. Intelligent and efficient management technologies will be used to implement automation, integration, centralization, and intelligence in power grid management, such as power generation, transmission, distribution, and energy consumption [2]. As an important connection hub in the power supply network, the substation needs regular inspection in order to find potential problems in time and maintain them in time to ensure the safe operation of the power grid [3]. As an important carrier of automatic monitoring of substation operation, robot can be widely used in the automatic monitoring of substation environment [4]. The magnetic path navigation method is simple and reliable and has high navigation accuracy, but this method uses a magnetic path for navigation, which requires a change in the layout of the substation. There are cargo and potential safety hazards during actual work [5]. Inertial navigation and wireless positioning methods require the installation of wireless devices for signal transmission and reception in the work environment. Although the installation is convenient, the decentralized wireless devices lead to poor recognition stability and adaptability and are prone to cumulative errors [6, 7]. Although GPS navigation method can work without adjusting the working scene, it has poor accuracy and low accuracy. In particular, in the power system environment, electromagnetic interference is particularly strong, and the well cannot meet the accuracy requirements of substation patrol inspection [8]. Figure 1 shows a manufacturing technology of inspection robot based on improved LSTM+CNN algorithm.

2. Literature Review

The inspection system of electric power inspection robot is a scientific and technological achievement integrating multiple disciplines. In addition to the traditional and relatively perfect technologies such as machinery, electricians and

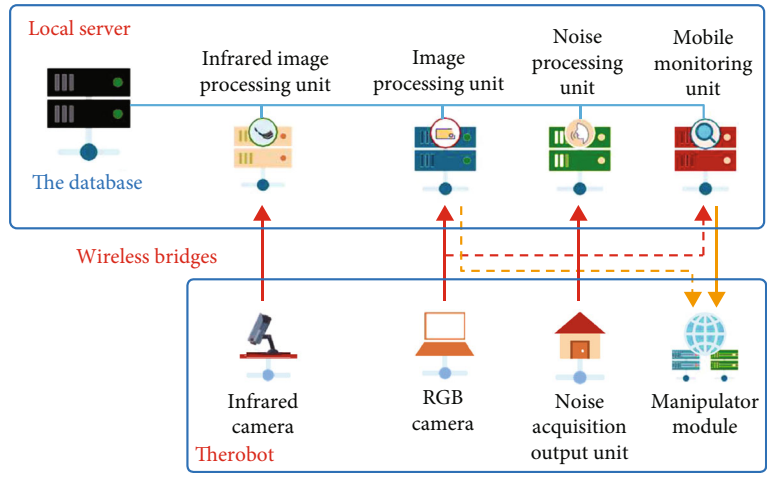

Figure 1: Manufacturing technology of inspection robot based on improved LSTM+CNN algorithm.

electronics, communication, automation, and sensors, it also adds deep learning neural network to improve the ability of system fault identification [9, 10]. The power inspection robot system is mainly composed of image detection and recognition unit, automatic obstacle avoidance unit, data monitoring unit, and data transmission and storage unit. The image detection system is a deep learning neural network based on PyTorch framework. It uses a neural network model similar to Yolov3 to dynamically collect image information, extract the characteristics of the image at any time, and judge whether there is fault information in the power system. Using this technology, the power inspection robot can directly warn the instrument panel, indicator lights, open fire, smoke, and other faults. At the same time, the video will be transmitted to the Alibaba cloud platform for backup, which can be retrieved by the inspectors at any time. It can also directly follow the real-time video and conduct video remote detection synchronously with the machine [11, 12]. Compared with the early inspection robot, the advantage of this power inspection robot is to increase the image detection function of convolutional neural network. Flexible neural networks are widely used in the field of visual target detection. Transient neural networks can automatically retrieve functional information from images, learn specific information from different lesion information, and continuously optimize their identification accuracy to effectively detect substations [13, 14]. The foreground vision device is used to capture the road image in real time, the image processing technology is used to identify the road surface to determine the position relationship between the inspection robot and the navigation line, and then the deep learning algorithm of the inspection robot walking and detection task is realized through the bottom motion control, which has attracted extensive attention in the existing visual path navigation methods [15]. Compared with other methods mentioned above, visual navigation method not only overcomes the disadvantages of low accuracy and poor adaptability of these methods in power system scene but also has the advantages of simplicity, reliability, accuracy, convenient transformation, and installation [16].

Based on this, we offer a reliable method of visual navigation for substation control robots to improve visual navigation performance in complex environments. This method uses the robustness of the gecko model (HM) to change the light, which solves the problem of compressing the navigation path in complex environments and reduces interference caused by external lighting factors. In order to effectively improve the accuracy of network recognition, semantic segmentation with a deep neural network (DCNN) based on a preprocessed image of HM is obtained, which provides information on global features, local features, and multiscale images.

3. Research Methods

3.1. Color Space Conversion. Good road recognition ability is the key to the self-adaptive navigation of the substation inspection robot. Only by controlling the inspection robot on the basis of identifying the effective road surface can the inspection robot effectively complete the inspection task and avoid entering the restricted area or areas that are not suitable for driving. Road recognition based on camera images needs to take into account various complex situations such as strong light, shadows, and rainy days. Define the maximum value of the three component values of R, G, and B of each pixel (i, j) as $\max(i, j)$ and the minimum value as $\min(i, j)$, and then, there are

$$\max(i, j) = \max(R(i, j), G(i, j), B(i, j)), \tag{1}$$

$$\min(i, j) = \min(R(i, j), G(i, j), B(i, j)). \tag{2}$$

For the three components in HM, V component represents color brightness, and $V(i, j)$ is expressed as

$$V(i, j) = \max(i, j). \tag{3}$$

S component represents color purity, and then, $S(i, j)$ represents

$$S(i,j) = \begin{cases} \dfrac{V(i,j) - \min(i,j)}{V(i,j)} V(i,j) \neq 0, \\ 0 V(i,j) = 0. \end{cases} \tag{4}$$

3.2. Gray Image Reconstruction. Each component of the Hopfield Model (HM) has different characteristics. H, S, and V components of different weights are reassembled to restore the image to minimize the effect of lighting changes in the image [17, 18]. In terms of features, the navigation path properties on components H and V are essentially opposite; the normalization method is considered to enhance and preliminarily extract the navigation path feature information. First, inverse image processing is performed on the H component, as shown in

$$\bar{H}(i,j) = 255 - H(i,j). \tag{5}$$

Then, the inverse image $\bar{H}$ is normalized, where the normalized range is $[a, b]$, where a is the minimum value of H and b is the maximum value of H, and then, the corresponding coefficient matrix H' is obtained, as shown in

$$H'(i,j) = \bar{H}(i,j) \times \frac{(b-a)}{255} + \frac{a}{255}. \tag{6}$$

This operation avoids the forced enlargement and reduction of the image in the normalization process. To recreate the gray image, add the components to the components and then multiply by a coefficient matrix according to

$$F(i,j) = (2 \times S(i,j) + V(i,j)) \times H'(i,j). \tag{7}$$

Analyze equation (7) and select the components of the reconstructed gray image and double the result. Consider effectively eliminating shadow interference in the image by increasing the weight of the components while restoring the gray image. This allows you to restore a gray image without the interference of external objects such as strong light, shadows, and surface water that highlight the road surface [19].

3.3. Image Acquisition under Dark Light Conditions. In the dark light environment, due to the light supplement defect of the point light source of the ordinary light source, the image acquisition of the inspection robot has light spots or concentrated light points, which brings the influence of image acquisition. Based on the HM, the image components are decomposed and used to detect the brightness of a simple light source, and the illumination of the collected image under the condition of dark light is appropriately adjusted. If the average brightness in the V component is defined as V_P, then equation (8) is shown.

$$V_P = \frac{\sum_{i=0}^{255} i \times v(i)}{\sum_{i=0}^{255} v(i)}, \tag{8}$$

where i is the saturation value of component s and $s(i)$ is the number of pixels in the saturation value. Define the average illuminance of the component as SP, followed by

$$S_P = \frac{\sum_{i=0}^{255} i \times s(i)}{\sum_{i=0}^{255} s(i)}, \tag{9}$$

where i is the saturation value in the S component and $s(i)$ is the pixel count in the saturation value. In combination with equations (8) and (9), the conditions for judging whether the image is too bright or too dark are (a) $V_P > 150$ and $S_P < 80$ and (b) $V_P < 75$ and $S_P > 60$.

According to the above results, the inspection robot analyzes the brightness information in the current image and determines whether the supplementary light intensity needs to be adjusted so that the light intensity can reach the same illuminance during path navigation in different road sections, so as to ensure the consistency and stability of the image collected by the camera [20, 21].

3.4. HM-DCNN. For a traditional CNN extension, the DCNN structure still consists of a circulation layer, a sampling layer, a consolidation layer, and a fully connected layer. Different from other conventional road semantic segmentation networks, HM-DCNN proposed in this paper performs semantic segmentation of the image through deep learning after image gray preprocessing, adding the adjustment of different light source intensity and supplementary preprocessing layer. In addition, because the preprocessed image is more concise and unified, the complexity of the network and the scale of target training parameters can be greatly reduced. The specific algorithm flow of the improved HM-DCNN is as follows. Based on the HM, complete the image acquisition and corresponding gray image reconstruction under the light conditions of different light sources, and adjust the fill light intensity appropriately. Through the first CNN, the global location is carried out to find the feature point region of continuous features and local features, and then, the maximum rectangular region of the target and surrounding objects is output. The convolutional layer is a key component of the HM-DCNN, and its primary function is to calculate the multiplication of the receiving field point and the rotation of the filter (or core) that can be studied. After the conversion operation, a nonlinear sample is performed in the aggregation layer to reduce the dimensionality of the data [22, 23]. The most common integration strategy is the most consolidated and average consolidation. Max pooling takes the maximum value from the candidates, while the average aggregation selects the average from the estimated candidates. Here, the maximum aggregation method is chosen to minimize the calculated average displacement due to the rotation layer parameter error in order to preserve the image structure information as much as possible. The function map obtained after the sample below is then sent to the activation function to process the nonlinear

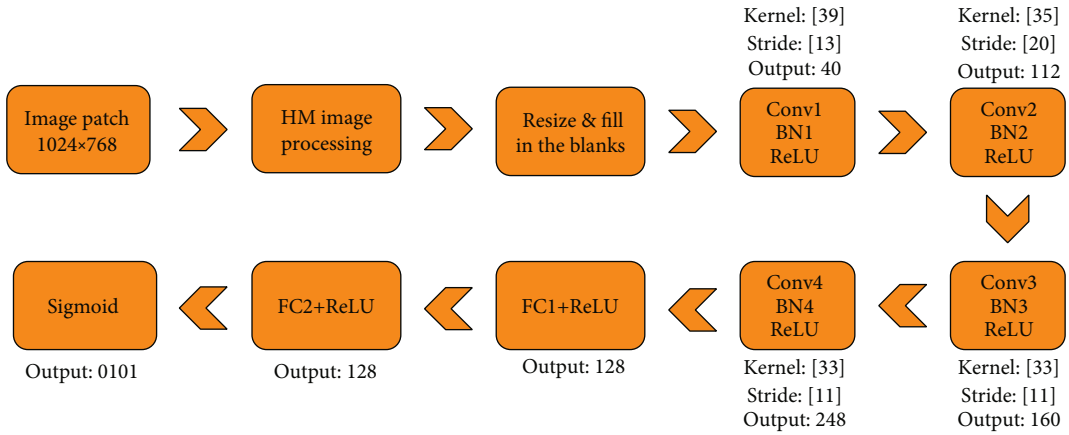

Figure 2: DCNN architecture.

Table 1: Network parameter settings.

Type	Convolution kernel parameters	Output
Convolution 1	Kernel: [3 9], stride: [1 3], output: 40	46 × 62 × 40
Max-pool 1	Kernel: [2 3], stride: 2	23 × 31 × 40
Convolution 2	Kernel: [3 9], stride: [1 3], output: 40	25 × 27 × 112
Max-pool 2	Kernel: [2 3], stride: 2	13 × 13 × 112
Convolution 3	Kernel: [3 3], stride: [1 1], output: 160	13 × 13 × 160
Convolution 4	Kernel: [3 3], stride: [1 1], output: 128	13 × 13 × 128
Max-pool 3	Kernel: [3 3], stride: 2	6 × 6 × 128
FC 1	Output: 128	128
FC 2	Output: 128	128

conversion. High-level grounding is done through fully connected layers. Nerve cells in this layer are involved in all the activations of the previous layer. The loss layer is usually the last layer of the DCNN and specifies how to punish the difference between the predicted and actual label during network training. Distribution points are strongly separated by a sigmoid layer. Here, a complete circulatory neural network based on the BVLC Caffe was selected to generate the HM-DCNN. The network structure is shown in Figure 2. There are a total of five circulation layers between the input and output layers. The network uses the Linear Unit (ReLU) as a function of nonlinear activation and finally identifies the distribution points of semantic segmentation through the sigmoid and builds the corresponding DCNN architecture. Table 1 shows the parameters for generating the corresponding circulation network according to the functional definition of the different layers of the DCNN [24].

Due to grayscale reconstruction preprocessing in the inspection robot, global gain normalization is applied to the processed images to further reduce the intensity changes in the images. This gain is calculated by aligning the calculated signal envelope using the median filter. To calculate the signal envelope, the image is filtered through a low-pass Gaussian core. DCNN is highly resistant to lighting changes, but the combination of image gray recovery and normal processing makes the signal dynamic range more uniform, which can further improve processing accuracy and merging speed.

Table 2: Lighting effect.

Scene	V_P	S_P	Effect
A	160.2	30.4	Normal
B	94.6	65	Suitable
C	60.2	103.5	Dark

4. Result Analysis

4.1. HM Fill Light Experiment and Image Preprocessing. To test the effectiveness of the proposed HM-DCNN network application in combination with the gray reconstruction in the actual substation scene, the substation path map collected by the substation control robot was used to train the network and test the network recognition accuracy. The network was trained in stochastic gradient drop (SGD), and the learning speed was set to 0.01, the pulse parameter to 0.9, and the weight loss to 0.0005. In order to make the inspection robot still run well in the dark environment, it is particularly important to supplement the light

Table 3: Influence of different light intensity and light supplement on detection accuracy.

Algorithm	Average coverage accuracy of normal light	Average accuracy of dim light	Under fill light condition
VGG	0.863	0.832	0.846
HM-VGG	0.87	0.860	0.860
SCNN	0.940	0.886	0.910
HM-SCNN	0.941	0.910	0.915
BiseNet	0.935	0.900	0.920
HM-BiseNet	0.930	0.916	0.914
DCNN	0.950	0.878	0.900
HM-DCNN	0.952	0.942	0.948

appropriately. Scene A is the road condition during the day, scene B is the adaptive fill light condition, and scene C is the nonfill light condition. The calculation results of V_P and S_P are shown in Table 2.

From the results in Table 2, it can be seen that the differences between the V_P and S_P components are clear in different lighting conditions. According to different difference values, setting the corresponding threshold can achieve appropriate light compensation. In order to analyze the influence of HM on the network recognition effect in the scene, the traditional edge extraction processing alone has poor adaptability in the case of high illumination difference and scene feature brightness and will lose a lot of details. The image after HM color space conversion and gray reconstruction can compress the color space and greatly retain the edge detail features, which is conducive to further scene pavement recognition by semantic segmentation network.

4.2. HM-DCNN Semantic Segmentation Experiment. In the preparation process of HM-DCNN training samples, in order to avoid the overfitting of training, improve the robustness of the network, and better extract the core features, a series of adjustments are made to the sample data, including illumination, color saturation, rotation, and clipping.

As a user-defined layer of other reasoning network preprocessing, HM can be combined with a variety of semantic segmentation networks. The processed image is used for gray reconstruction, which is used as the input of each comparison network and compared with the network results trained with the original image directly as the input. The effects of different illumination conditions on the experimental results are shown in Table 3.

As shown in Figure 3, the recognition effects of several commonly used semantic segmentation networks are compared and analyzed through experiments. Under normal illumination, DCNN has high recognition effect, but under dim illumination and supplementary illumination, the recognition effect decreases significantly. Through the comparison of each network after adding HM treatment, although the improvement effect under normal light is not significant, the recognition rate of the dark environment of the original network has been greatly improved, especially when combined with DCNN.

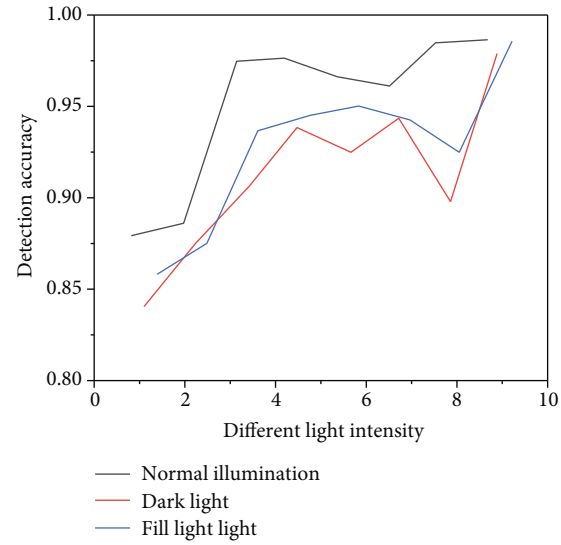

Figure 3: Influence of different light intensity and light supplement on detection accuracy.

Table 4: Comparison of model size and reasoning speed of different recognition networks.

Algorithm	Model size (MB)	Average error (%)	Embedded reasoning time (ms)
VGG	400	84.7	300
SCNN	157	91.2	160
HM-SCNN	158	92.2	120
BiseNet	55	91.8	110
HM-BiseNet	57	92.0	98
DCNN	45	90.9	90
HM-DCNN	47	94.7	78

As shown in Table 4, the original structure of the network is not adjusted and the corresponding preprocessing layer is added, which makes the size of the network model increase relatively, but the reasoning speed of the original network is significantly improved, with an average of 16.4%.

5. Conclusion

This document proposes a new method of reliable visual navigation of substation control robots in complex road environments, which has the advantages of strong anti-interference ability, simple operation, high precision, and good stability. This method fully considers the road characteristics and working conditions of the substation and uses the insensitivity of HM color space to light change, shadow, and interference to reconstruct the gray image of the collected image; therefore, the specifics of the navigation path are reflected in more detail. In addition, DCNN is used to train and recognize images processed on a grayscale to improve network recognition accuracy. Because the HM reduces the amount of color space, the first-ever DCNN

can be used in substation control robots with poor processing capabilities. The results of the experiment show that the network recognition results show a clear advantage in combination with the HM gray reconstruction compared to the existing pure training network. At the same time, the HM-DCNN method proposed in this paper can stabilize the average processing accuracy of DCNN from 91% to 93%, have the best effect on the entire network, and fully meet the actual needs of the substation situation.

Data Availability

The data used to support the findings of this study are available from the corresponding author upon request.

Conflicts of Interest

The authors declare that they have no conflicts of interest.

References

[1] O. Abdel Wahab, A. Mourad, H. Otrok, and T. Taleb, "Federated machine learning: survey, multi-level classification, desirable criteria and future directions in communication and networking systems," *IEEE Communications Surveys & Tutorials*, vol. 23, no. 2, 2021.

[2] A. Mourad, A. Srour, H. Harmanani, C. Jenainati, and M. Arafeh, "Critical impact of social networks infodemic on defeating coronavirus COVID-19 pandemic: twitter-based study and research directions," *IEEE Transactions on Network and Service Management*, vol. 17, no. 4, 2020.

[3] M. W. Kim, S. Lee, I. Dan, and S. Tak, "A deep convolutional neural network for estimating hemodynamic response function with reduction of motion artifacts in fnirs," *Journal of Neural Engineering*, vol. 19, no. 1, article 016017, 2022.

[4] X. Zheng and Z. Cai, "Privacy-preserved data sharing towards multiple parties in industrial IoTs," *IEEE Journal on Selected Areas in Communications (JSAC)*, vol. 38, no. 5, pp. 968–979, 2020.

[5] J. Qiu, L. Du, D. Zhang, S. Su, and Z. Tian, "Nei-TTE: intelligent traffic time estimation based on fine-grained time derivation of road segments for smart city," *IEEE Transactions on Industrial Informatics*, vol. 16, no. 4, pp. 2659–2666, 2020.

[6] R. M. Churchill, B. Tobias, Y. Zhu, and DIII-D team, "Deep convolutional neural networks for multi-scale time-series classification and application to tokamak disruption prediction using raw, high temporal resolution diagnostic data," *Physics of Plasmas*, vol. 27, no. 6, article 062510, 2020.

[7] Z. Lv, W. Kong, X. Zhang, D. Jiang, H. Lv, and X. Lu, "Intelligent security planning for regional distributed energy internet," *IEEE Transactions on Industrial Informatics*, vol. 16, no. 5, pp. 3540–3547, 2020.

[8] Z. Lv, L. Qiao, J. Li, and H. Song, "Deep-learning-enabled security issues in the Internet of things," *IEEE Internet of Things Journal*, vol. 8, no. 12, pp. 9531–9538, 2021.

[9] S. Mekruksavanich and A. Jitpattanakul, "Deep convolutional neural network with rnns for complex activity recognition using wrist-worn wearable sensor data," *Electronics*, vol. 10, no. 14, p. 1685, 2021.

[10] F. Wu, B. Wu, M. Zhang, H. Zeng, and F. Tian, "Identification of crop type in crowdsourced road view photos with deep convolutional neural network," *Sensors*, vol. 21, no. 4, p. 1165, 2021.

[11] S. Kim and H. Kim, "Zero-centered fixed-point quantization with iterative retraining for deep convolutional neural network-based object detectors," *IEEE Access*, vol. 9, pp. 20828–20839, 2021.

[12] L. Song, H. Wang, and P. Chen, "Automatic patrol and inspection method for machinery diagnosis robot—sound signal-based fuzzy search approach," *IEEE Sensors Journal*, vol. 20, no. 15, pp. 8276–8286, 2020.

[13] V. Muthugala, P. Palanisamy, B. Samarakoon, S. Padmanabha, and D. N. Terntzer, "Raptor: a design of a drain inspection robot," *Sensors*, vol. 21, no. 17, p. 5742, 2021.

[14] X. Cheng, B. Yang, A. Hedman, T. Olofsson, H. Li, and L. Van Gool, "NIDL: a pilot study of contactless measurement of skin temperature for intelligent building," *Energy and Buildings*, vol. 198, pp. 340–352, 2019.

[15] S. Yang, B. Deng, J. Wang et al., "Scalable digital neuromorphic architecture for large-scale biophysically meaningful neural network with multi-compartment neurons," *IEEE transactions on neural networks and learning systems*, vol. 31, no. 1, pp. 148–162, 2020.

[16] B. Zhang, J. Wu, L. Wang, and Z. Yu, "Accurate dynamic modeling and control parameters design of an industrial hybrid spray-painting robot," *Robotics and Computer-Integrated Manufacturing*, vol. 63, no. 1, article 101923, 2020.

[17] M. Muthugala, K. Apuroop, S. Padmanabha, S. Samarakoon, and R. Wen, "Falcon: a false ceiling inspection robot," *Sensors*, vol. 21, no. 16, p. 5281, 2021.

[18] R. Parween, Y. W. Tan, and M. R. Elara, "Design and development of a vertical propagation robot for inspection of flat and curved surfaces," *IEEE Access*, vol. 9, pp. 26168–26176, 2021.

[19] R. G. Lins and S. N. Givigi, "Fpga-based design optimization in autonomous robot systems for inspection of civil infrastructure," *IEEE Systems Journal*, vol. 14, no. 2, pp. 2961–2964, 2020.

[20] T. Zhang, G. Han, C. Lin, N. Guizani, and L. Shu, "Integration of communication, positioning, navigation and timing for deep-sea vehicles," *IEEE Network*, vol. 34, no. 2, pp. 121–127, 2020.

[21] X. Zhou, X. Xu, W. Liang et al., "Intelligent small object detection for digital twin in smart manufacturing with industrial cyber-physical systems," *IEEE Transactions on Industrial Informatics*, vol. 18, no. 2, pp. 1377–1386, 2022.

[22] J. Wang, J. Liu, X. Xu, Z. Yu, and Z. Li, "A single foot-mounted pedestrian navigation algorithm based on the maximum gait displacement constraint in three-dimensional space," *Measurement Science and Technology*, vol. 33, no. 5, p. 055113, 2022.

[23] F. Potortì, F. Palumbo, and A. Crivello, "Sensors and sensing technologies for indoor positioning and indoor navigation," *Sensors*, vol. 20, no. 20, p. 5924, 2020.

[24] X. Zhou, W. Liang, K. Wang, R. Huang, and Q. Jin, "Academic influence aware and multidimensional network analysis for research collaboration navigation based on scholarly big data," *IEEE Transactions on Emerging Topics in Computing*, vol. 9, no. 1, pp. 246–257, 2021.